




Optics Letters

Simultaneous turbulence mitigation and channel demultiplexing for two 100 Gbit/s orbital-angular-momentum multiplexed beams by adaptive wavefront shaping and diffusing

RUNZHOU ZHANG,^{1,*}  HAO SONG,¹ ZHE ZHAO,¹ HAOQIAN SONG,¹ JING DU,¹ CONG LIU,¹  KAI PANG,¹ LONG LI,¹ HUIBIN ZHOU,¹ ARI N. WILLNER,¹ AHMED ALMAIMAN,^{1,2}  YIYU ZHOU,³ ROBERT W. BOYD,³ BRITTANY LYNN,⁴ ROBERT BOCK,⁵ MOSHE TUR,⁶ AND ALAN E. WILLNER¹

¹Department of Electrical Engineering, University of Southern California, Los Angeles, California 90089, USA

²King Saudi University, Riyadh 11362, Saudi Arabia

³Institute of Optics, University of Rochester, Rochester, New York 14627, USA

⁴Space & Naval Warfare Systems Center, Pacific, San Diego, California 92152, USA

⁵R-DEX System, Marietta, Georgia 30068, USA

⁶School of Electrical Engineering, Tel Aviv University, Ramat Aviv 69978, Israel

*Corresponding author: runzhou@usc.edu

Received 20 November 2019; revised 21 December 2019; accepted 24 December 2019; posted 24 December 2019 (Doc. ID 383714); published 30 January 2020

We experimentally demonstrate simultaneous turbulence mitigation and channel demultiplexing in a 200 Gbit/s orbital-angular-momentum (OAM) multiplexed link by adaptive wavefront shaping and diffusing (WSD) the light beams. Different realizations of two emulated turbulence strengths (the Fried parameter $r_0 = 0.4, 1.0$ mm) are mitigated. The experimental results show the following. (1) Crosstalk between OAM $l = +1$ and $l = -1$ modes can be reduced by >10.0 and >5.8 dB, respectively, under the weaker turbulence ($r_0 = 1.0$ mm); crosstalk is further improved by >17.7 and >19.4 dB, respectively, under most realizations in the stronger turbulence ($r_0 = 0.4$ mm). (2) The optical signal-to-noise ratio penalties for the bit error rate performance are measured to be ~ 0.7 and ~ 1.6 dB under weaker turbulence, while measured to be ~ 3.2 and ~ 1.8 dB under stronger turbulence for OAM $l = +1$ and $l = -1$ mode, respectively. © 2020 Optical Society of America

<https://doi.org/10.1364/OL.383714>

Due in part to the desire for more bandwidth between different kinds of platforms, there is keen interest in increasing the data transmission capacity of free-space optical (FSO) communication links [1]. One potential approach for capacity enhancement is to use a form of space-division multiplexing known as mode-division-multiplexing (MDM) [2]. In mode multiplexing, multiple independent data-carrying beams are simultaneously transmitted through a single transmitter (Tx) and receiver (Rx) aperture pair, such that each beam can be described as a unique mode from an orthogonal modal basis set. The orthogonality among different beams enables efficient

multiplexing, co-axial propagation, and demultiplexing with little inherent crosstalk (XT) [3].

As one example, FSO MDM links can utilize orbital-angular-momentum (OAM) modes, which are a subset of the Laguerre–Gaussian (LG) modal basis set [4]. A propagating OAM beam has a phase front that twists in helical fashion. The amount of carried OAM is represented by an integer l , which is the number of 2π phase shift in the wavefront. The intensity profile of such an OAM beam is a ring-shaped “doughnut” with little power at its center [5].

In an OAM FSO transmission system, the link tends to have little dispersive effect, but suffers from beam divergence [6] and atmospheric turbulence [7]. Turbulence effect is a significant challenge, because it can induce modal power coupling and resultant inter-channel XT [7]. Mitigation of turbulence in OAM links has been demonstrated using (1) adaptive optics that corrects the distorted wavefront [8] and (2) multiple-input-multiple-output electronic digital signal processing [9].

An additional challenge for OAM FSO links is to efficiently demultiplex multiple spatial modes [10–12]. Recently, an approach for OAM demultiplexing used adaptive wavefront shaping and diffusing (WSD) of different modes [13]. Multiple OAM modes are shaped to interact differently with a deterministic multiple-scattering medium, such that the scattered light from different modes can be separated to different spatial locations.

In this Letter, we experimentally exploit WSD [14] to tackle the above two issues and to achieve simultaneous turbulence mitigation and mode demultiplexing for a 200 Gbit/s OAM multiplexed FSO link. Two OAM $l = +1$ and $l = -1$ modes, each carrying a 100 Gbit/s quadrature phase shift keying

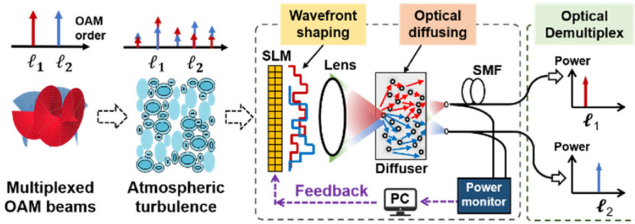


Fig. 1. Concept of using WSD to mitigate the turbulence effects and simultaneously demultiplex two data-carrying OAM beams.

(QPSK) signal, are multiplexed and transmitted through emulated atmospheric turbulence. Two different turbulence strengths (TSs) with the Fried parameters $r_0 = 0.4$ mm (stronger) and $r_0 = 1.0$ mm (weaker) are emulated. Using WSD, we mitigate turbulence-induced beam distortion as large as $D/r_0 = 6.0$ (the ratio of the beam size to the Fried parameter). The experimental results for OAM $l = +1$ and $l = -1$ modes show the following: (1) XT is reduced by >10.0 and >5.8 dB under the weaker turbulence conditions and by >17.7 and >19.4 dB for most realizations of a stronger turbulence scenario, respectively, and (2) a bit error rate (BER) performance below the $3.8e-3$ forward error correction (FEC) limit is achieved under different turbulence conditions. Optical signal-to-noise (OSNR) penalties at the FEC limit for the OAM $l = +1$ and $l = -1$ modes are measured as ~ 0.7 and ~ 1.6 dB for weaker turbulence, while measured to be ~ 3.2 and ~ 1.8 dB for stronger turbulence, respectively.

As shown in Fig. 1, two pure orthogonal OAM modes are distorted by atmospheric turbulence, which couples the power of each OAM mode into many neighboring spatial modes [7]. In an OAM multiplexed link, such power coupling leads to inter-channel XT and degrades the system performance. The atmospheric turbulence is emulated by a single-phase screen, whose random transfer function $U(x, y) = \exp(i\psi(x, y))$ multiplies the incident fields, $E_1(x, y)$ and $E_2(x, y)$, causing them to couple together upon reception if demultiplexed using their original OAM modal basis. Without the turbulence effects, a WSD system has been utilized to separate multiple pure OAM modes by shaping the beams with a specific phase front [13]. One can modify such a phase front in WSD so that it can also act as an inverse transfer function $U^*(x, y) = \exp(-i\psi(x, y))$ for that of turbulence [14]. Therefore, WSD can perform turbulence mitigation and channel demultiplexing simultaneously. The performance of WSD may depend on the received portion of the distorted beams. If only partial optical beams are collected by the Rx aperture, the system performance might be degraded by extra modal XT due to limited aperture effects [6]. In WSD, these distorted wavefronts are then shaped by a phase-only spatial light modulator (SLM) and focused onto an optical diffuser in which the light fields are scattered multiple times. Generally, such a multiple-scattering process may further degrade the mode purities of the OAM beams [15]. However, by applying the “correct” phase pattern on the SLM, WSD can be mode-selective so that light fields from different distorted OAM modes would experience different scattering trajectories inside the diffuser; then the fields emerging from the diffuser are refocused to different spatial locations [13,16] and collected by single-mode fibers (SMFs).

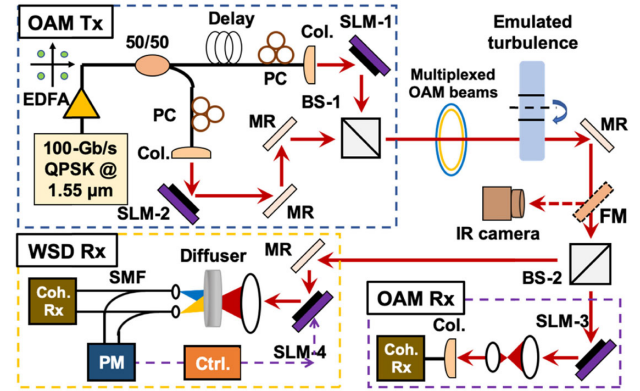


Fig. 2. Experimental setup of using WSD to mitigate turbulence effects in a 200 Gbit/s OAM multiplexed link. PC, polarization controller; FM, flip mirror; MR, mirror; PM, power meter; Ctrl., controller.

Figure 2 shows the experimental setup. At the Tx, a 100 Gbit/s QPSK signal is generated at ~ 1.55 μm using an in-phase quadrature (IQ) modulator. It is then amplified by an erbium-doped fiber amplifier (EDFA) and sent into a 50/50 fiber coupler. One of the two copies is delayed by a ~ 1 m SMF to decorrelate the data sequences, and both copies are coupled to free space via SMF collimators (Col.). These two optical beams are launched onto SLM-1 and SLM-2 to convert them to OAM $l = +1$ and $l = -1$ mode (beam size ~ 2.4 mm), respectively. A beam splitter (BS-1) multiplexes the data-carrying OAM $l = \pm 1$ beams, and the resultant beams are transmitted through the emulated turbulence. The atmospheric turbulence is emulated by (static) thin phase screen plates which are designed to produce Kolmogorov spectrum statistics with the effective Fried coherence length $r_0 = 0.4, 1.0$ mm, respectively [7,17]. Different realizations of emulated turbulence are implemented by rotating the plate to different orientations. A dimensionless measure for beam distortion of an optical beam is defined as the ratio of the beam size to the Fried coherence length, i.e., D/r_0 . Based on the selected r_0 , we emulate different levels of beam distortion induced by different TSs: no turbulence ($D/r_0 = 0$), weaker turbulence ($D/r_0 = 2.4$), and stronger turbulence ($D/r_0 = 6.0$), denoted as TS-0, TS-1, and TS-2, respectively. At the Rx, the distorted beams are equally split by BS-2. One branch is sent to a normal OAM Rx [4] for measuring the modal XT induced by the emulated turbulence. For this purpose, SLM-3 is loaded with a phase pattern conjugate to the OAM mode of interest. The other branch sends the two modes to the WSD Rx. For each turbulence realization, the wavefront of the distorted beams is first shaped by SLM-4 and then focused by a lens ($f = 50$ mm) onto an optical diffuser (ground glass with grit 120, Thorlabs). A pair of SMFs, spaced apart by 127 μm , is placed ~ 1 mm behind the diffuser. The collected power for each SMF port is fed to the SLM-4 controller in which a genetic algorithm (GA) (MATLAB global optimization toolbox) is applied to search for the SLM-4-loaded phase pattern that aims to maximize the received power of each distorted OAM mode. These SMFs, each carrying (ideally) a single data stream, are then connected to individual coherent Rxs for error-free data recovery.

Figure 3(a) shows the intensity profiles of the received OAM $l = +1$ beam affected by the different TSs. As shown

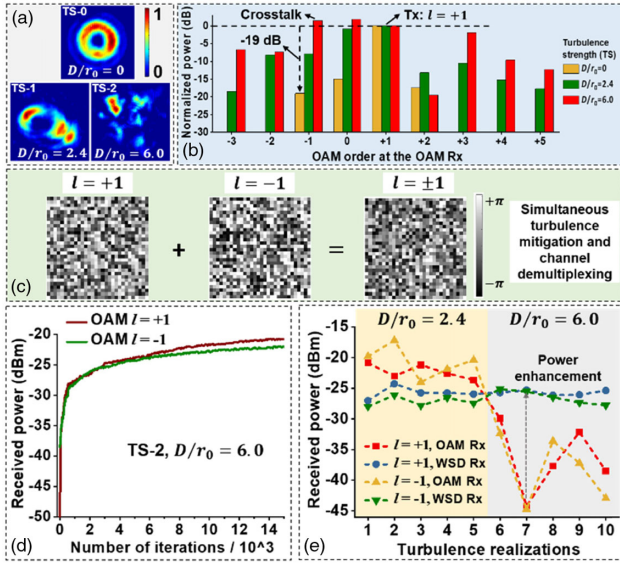


Fig. 3. (a) Turbulence-distorted OAM $l = +1$ beam profiles; (b) received OAM spectrum of the distorted $l = +1$ beam; (c) one example of the determined 30×30 phase pattern; (d) received power of each mode versus the number of iterations during the wavefront shaping process; (e) received power of each mode after WSD mitigates different turbulence realizations (TS-1, realization 1–5; TS-2, realization 6–10).

in Fig. 3(b), the ratio of leakage power to the neighboring OAM modes ($l = 0$ and $l = +2$) is as low as ~ -15 dB under TS-0. However, the power of the transmitted OAM $l = +1$ mode spreads to many other modes under turbulence effects. For instance, the ratio of the power coupled to the OAM $l = -1$ mode increases from -19.04 dB (TS-0) to -7.94 and 1.51 dB under the effects of TS-1 and TS-2, respectively. Turbulence-induced distortion depends on both the realization and strength of the emulated turbulence. In WSD, each turbulence realization with different strengths requires searching for a wavefront-shaping phase pattern. One example of the optimized phase pattern is shown in Fig. 3(c), which consists of 30×30 elements, each of which occupies 20×20 pixels of the SLM-4. The wavefront-shaping process for each turbulence realization in WSD consists of two steps. The first step is to transmit one OAM beam through the emulated turbulence at a time and independently maximize the received power at the designated SMF. Thus, two different phase patterns θ_1 and θ_2 can be determined for OAM $l = +1$ and $l = -1$ mode, respectively. The second step is to apply the phase pattern given by $\theta = \arg[\exp(i\theta_1) + \exp(i\theta_2)]$ to simultaneously mitigate the turbulence effect and demultiplex the $l = \pm 1$ modes [18]. As shown in Fig. 3(d), the received powers of the distorted OAM $l = +1$ and $l = -1$ modes (under TS-2) converge to ~ -20.7 and ~ -21.9 dBm, respectively, after ~ 15000 measurement iterations. In this demonstration, each iteration of WSD takes ~ 0.1 s, and the GA takes ~ 1200 s to converge to the desired output. Although such a speed is mainly limited by the refresh rate of the SLM (~ 10 Hz), we believe that the operation time of WSD can be significantly reduced by using faster-responding devices [16]. If the mitigation pattern is fixed, the operation speed of WSD needs to be accelerated to keep the

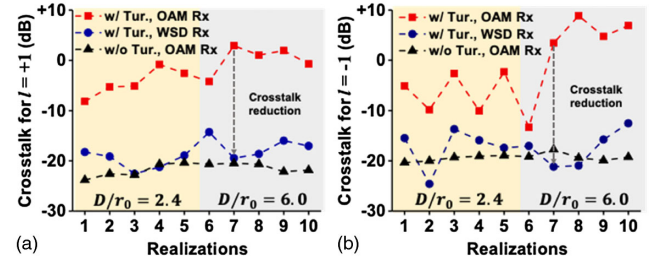


Fig. 4. Measured XT using OAM and WSD Rx for receiving distorted OAM modes: (a) $l = +1$ mode and (b) $l = -1$ mode. The XT without turbulence effects using OAM Rx is also shown. Tur., turbulence.

BERs below the FEC threshold against the change of turbulence. For dynamic TS, we note that adaptively updating the phase pattern starting from a pre-optimized mitigation pattern may accelerate the GA's convergence and would likely be more time-efficient than starting from a blank phase pattern [19].

WSD is also applied to mitigate different realizations of TS-1 and TS-2. As shown in Fig. 3(e), under the effects of TS-2, the received powers of the $l = +1$ and $l = -1$ modes decrease by >6.25 and >8.41 dB, respectively. Here the stronger turbulence severely distorts the beams' wavefronts and, consequently, induces more modal power coupling. After WSD is applied to mitigate realizations 1–5 of the weaker turbulence, 1–6 and 3–8 dB MDL, respectively, are observed for receiving the $l = +1$ and $l = -1$ modes. However, as for the realizations 6–10 of stronger turbulence, WSD is capable of enhancing the received power $\sim 4 - 19$ dB for the two modes. This may be because WSD controls a large number of spatial modes and, thus, may couple some of the leakage power back to the received mode [16]. Moreover, the WSD-mitigated powers for both modes are ~ -26 dBm for realizations 1–10, not significantly depending on the realizations.

XT improvement for receiving the two OAM modes using WSD is shown in Fig. 4. For comparison, the XT for receiving both the OAM modes using the OAM Rx under TS-0 is ~ -20 dB. Such XT slightly fluctuates over time due to the drift of alignments in the OAM multiplexed link. Under TS-1, the XT for the $l = +1$ and $l = -1$ modes can be suppressed by >10.0 and >5.8 dB, respectively. XTs can also be reduced by >17.7 dB under TS-2 for realizations 7–10. It also appears that the mitigation performance of WSD does not largely depend on the turbulence realizations. We note that the mitigated XT may be even lower than the XT without turbulence effects. For example, the XT for OAM $l = -1$ is decreased from $+3.41$ to -21.17 dB (realization 7), which is lower than the XT without turbulence, that is, -17.72 dB (using OAM Rx). This may be because WSD also corrects some misalignment of the optical link and, thus, further decreases the XT.

Figure 5 shows the measured BER as a function of the OSNR after WSD mitigates different turbulence effects. Without any turbulence effects (TS-0), BER values for both modes using the normal OAM Rx easily fall below the 7% FEC limit. However, using the OAM Rx under TS-1, a power penalty as large as ~ 9.3 dB at the FEC limit is observed for decoding $l = +1$ mode and the $l = -1$ mode cannot achieve below the FEC limit, shown in Figs. 5(a) and 5(b), respectively. For the case of TS-2, both OAM modes can hardly achieve below the FEC limit due

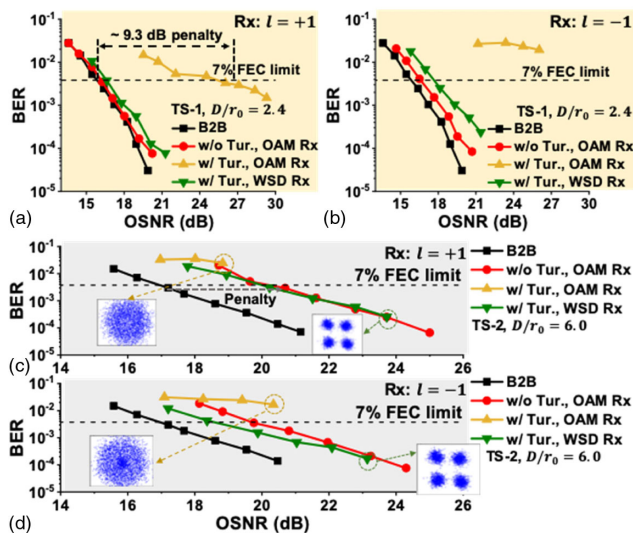


Fig. 5. Measured BER of OAM-carried data channel as a function of OSNR under different turbulence effects: (a) $l = +1$ under TS-1; (b) $l = -1$ under TS-1; (c) $l = +1$ under TS-2; (d) $l = -1$ under TS-2.

to the presence of strong XT between these two channels, shown in Figs. 5(c) and 5(d). After WSD is applied to mitigate the turbulence effects, both distorted modes exhibit similar BER performances as the BER performance under TS-0, albeit with some OSNR penalties at the 7% FEC limit: ~ 0.7 and ~ 1.6 dB under TS-1, while ~ 3.2 and ~ 1.8 dB under TS-2 for the OAM $l = +1$ and $l = -1$ modes, respectively.

In general, turbulence mitigation approaches in FSO systems should be operated at a rate of \sim kilohertz [17]. We note that the operation speed of WSD can be potentially increased to \sim kilohertz level by (1) utilizing a high-speed wavefront modulator, e.g., a 350 kHz micro-electromechanical modulator in [20], and (2) applying a time-efficient algorithm, such as parallel wavefront optimization that reduces the number of measurements by more than an order of magnitude [21]. To enable OAM transmission over a longer distance (>100 m) in a field-trial link, several limiting factors need to be considered, including [6] (1) mode-dependent beam divergence effects, (2) power loss due to the limited aperture size, and (3) modal crosstalk induced by the misalignment between Tx and Rx. To accommodate extra OAM channels, one may need to consider (1) using low-loss mode multiplexer to reduce the $1/N$ combining loss [11,12], and (2) employing high-speed wavefront shaping algorithms and devices to reduce the extra operation time for demultiplexing more OAM channels [20,21]. Since turbulence is likely to induce little wavelength-dependent distortion, WSD might be potentially applicable in quantum communications by using an extra beacon on a separate wavelength [13,22].

Funding. National Science Foundation (ECCS-1509965); Air Force Research Laboratory (FA8650-18-P-1699); Vannevar

Bush Faculty Fellowship sponsored by the Basic Research Office of the Assistant Secretary of Defense (ASD) for Research and Engineering (RE); Office of Naval Research (N00014-16-1-2813); Defense Security Cooperation Agency (DSCA-4440646262).

Disclosures. The authors declare no conflicts of interest.

REFERENCES

1. Z. Ghassemlooy, S. Arnon, M. Uysal, Z. Xu, and J. Cheng, *IEEE J. Sel. Areas Commun.* **33**, 1738 (2015).
2. D. J. Richardson, J. M. Fini, and L. E. Nelson, *Nat. Photonics* **7**, 354 (2013).
3. S. Restuccia, D. Giovannini, G. Gibson, and M. Padgett, *Opt. Express* **24**, 27127 (2016).
4. J. Wang, J.-Y. Yang, I. M. Fazal, N. Ahmed, Y. Yan, H. Huang, Y. Ren, Y. Yue, S. Dolinar, M. Tur, and A. E. Willner, *Nat. Photonics* **6**, 488 (2012).
5. A. M. Yao and M. J. Padgett, *Adv. Opt. Photonics* **3**, 161 (2011).
6. G. Xie, L. Li, Y. Ren, H. Huang, Y. Yan, N. Ahmed, Z. Zhao, M. P. J. Lavery, N. Ashrafi, S. Ashrafi, R. Bock, M. Tur, A. F. Molisch, and A. E. Willner, *Optica* **2**, 357 (2015).
7. Y. Ren, H. Huang, G. Xie, N. Ahmed, Y. Yan, B. I. Erkmen, N. Chandrasekaran, M. P. J. Lavery, N. K. Steinhoff, M. Tur, S. Dolinar, M. Neifeld, M. J. Padgett, R. W. Boyd, J. H. Shapiro, and A. E. Willner, *Opt. Lett.* **38**, 4062 (2013).
8. Y. Ren, G. Xie, H. Huang, N. Ahmed, Y. Yan, L. Li, C. Bao, M. P. J. Lavery, M. Tur, M. A. Neifeld, R. W. Boyd, J. H. Shapiro, and A. E. Willner, *Optica* **1**, 376 (2014).
9. H. Huang, Y. Cao, G. Xie, Y. Ren, Y. Yan, C. Bao, N. Ahmed, M. A. Neifeld, S. J. Dolinar, and A. E. Willner, *Opt. Lett.* **39**, 4360 (2014).
10. G. Labroille, B. Denolle, P. Jian, P. Genevieux, N. Treps, and J.-F. Morizur, *Opt. Express* **22**, 15599 (2014).
11. N. K. Fontaine, R. Ryf, H. Chen, D. T. Neilson, K. Kim, and J. Carpenter, *Nat. Commun.* **10**, 1865 (2019).
12. G. C. G. Berkhout, M. P. J. Lavery, J. Courtial, M. W. Beijersbergen, and M. J. Padgett, *Phys. Rev. Lett.* **105**, 153601 (2010).
13. R. Fickler, M. Ginoya, and R. W. Boyd, *Phys. Rev. B* **95**, 161108 (2017).
14. R. Zhang, H. Song, Z. Zhao, H. Song, J. Du, C. Liu, K. Pang, L. Li, A. N. Willner, R. W. Boyd, M. Tur, and A. E. Willner, "Demonstration of independent turbulence mitigation of two 100 Gbit/s QPSK orbital-angular-momentum multiplexed beams using wavefront shaping and controlled scattering," in *Optical Fiber Communication Conference (OFC)*, San Diego, California, 3 March 2019, paper W4A.4.
15. R. Zhang, L. Li, Z. Zhao, G. Xie, G. Milione, H. Song, P. Liao, C. Liu, H. Song, K. Pang, A. N. Willner, B. Lynn, R. Bock, M. Tur, and A. E. Willner, *Opt. Lett.* **44**, 691 (2019).
16. I. M. Vellekoop and A. P. Mosk, *Opt. Lett.* **32**, 2309 (2007).
17. L. Andrews and R. Phillips, *Laser Beam Propagation through Random Media*, 2nd ed. (SPIE, 2005).
18. S. R. Huisman, T. J. Huisman, T. A. W. Wolterink, A. P. Mosk, and P. W. H. Pinkse, *Opt. Express* **23**, 3102 (2015).
19. I. M. Vellekoop and A. P. Mosk, *Opt. Commun.* **281**, 3071 (2008).
20. O. Tzang, E. Niv, S. Singh, S. Labouesse, G. Myatt, and R. Piestun, *Nat. Photonics* **13**, 788 (2019).
21. M. Cui, *Opt. Lett.* **36**, 870 (2011).
22. B. Rodenburg, M. Mirhosseini, M. Malik, O. S. Magaña-Loaiza, M. Yanakas, L. Maher, N. K. Steinhoff, G. A. Tyler, and R. W. Boyd, *New J. Phys.* **16**, 3 (2014).